GERMAN - MONGOLIAN INSTITUTE FOR RESOURCES AND TECHNOLOGY

The present work was submitted to

the German-Mongolian Institute of Resources and Technology

Design and Simulation of a Regenerative Braking System for Small Electric Vehicles

Bachelor's Thesis

By

Sumiyadorj Rentsennorov

Study program: Mechatronics Engineering

Student ID: B2100503

1st Supervisor/Examiner: Prof. Phd Sungchil Lee

2nd Supervisor/Examiner: Phd Kim Young Suk

Ulaanbaatar/Nalaikh

2025

GERMAN - MONGOLIAN INSTITUTE FOR RESOURCES AND TECHNOLOGY

The present work was submitted to

the German-Mongolian Institute of Resources and Technology

Design and Simulation of a Regenerative Braking System for Small Electric Vehicles

Bachelor's Thesis

By

Sumiyadorj Rentsennorov

Study program: Mechatronics Engineering

Student ID: B2100503

1st Supervisor/Examiner: Prof. Phd Sungchil Lee

2nd Supervisor/Examiner: Phd Kim Young Suk

Ulaanbaatar/Nalaikh

2025

Statutory Declaration

Rentsennorov Sumiyadorj	B2100503
Last Name, First Name	Student ID Number

I hereby affirm in lieu of an oath that I provided the submitted bachelor thesis

"Design and Simulation of a Regenerative Braking System for Small Electric Vehicles"

I did not use any sources other than those stated. In case that the work is additionally submitted on a data medium, I declare that the written and the electronic form are completely identical. The work was not submitted in the same or similar form to any examination authority.

May 28, 2025	
Place, Date	Signature

Table of Contents

List of Figures

Acknowledgement

I would like to sincerely thank Prof. Dr. Sungchil Lee and Dr. Kim Young Suk for accepting to be my supervisors and supporting the completion of this thesis. I am deeply grateful for their willingness to oversee my work and for their academic presence throughout the final stage of my studies.

I would also like to extend my appreciation to the faculty and staff of the German-Mongolian Institute for Resources and Technology (GMIT) for providing a strong academic foundation and access to laboratory facilities that enabled this research. Special thanks go to the instructors in the Mechatronics and Electrical Engineering departments, whose coursework and insights helped shape my understanding of simulation, energy systems, and control.

My thanks also go to my peers and classmates who offered support, encouragement, and helpful discussions during the research and prototyping process.

I am especially thankful to my family for their continuous support, motivation, and understanding throughout this academic journey. Their encouragement has been a source of strength and determination.

Lastly, I acknowledge the usefulness of open-source tools such as Arduino and MATLAB/Simulink, which were instrumental in developing and testing the system described in this thesis.

To everyone who played a part in this accomplishment,

Thank you.

Abstract

Small electric vehicles (SEVs), such as e-scooters and e-bikes, are becoming increasingly important for sustainable urban transport. However, their limited battery capacity significantly constrains range and usability, particularly in cities like Ulaanbaatar where cold weather and limited charging infrastructure further exacerbate these issues. This thesis investigates the design, simulation, and prototype testing of a regenerative braking system (RBS) specifically tailored for lightweight SEVs, with the goal of improving energy efficiency through kinetic energy recovery during deceleration.

The research begins with an exploration of the historical development and theoretical principles behind regenerative braking, including electromagnetic induction, Lenz's Law, and energy conservation. A simulation model was developed in MATLAB/Simulink to replicate a realistic SEV drivetrain using a 12V brushed DC motor, an H-bridge inverter, a lithium-ion battery, and a control logic system for modulating torque. Simulations were performed under both regenerative and non-regenerative scenarios. The results showed that when braking was applied, the system recovered approximately 4.48 joules of energy from 38.87 joules consumed, achieving an energy recovery efficiency of 11.52%. In contrast, the coasting scenario confirmed zero energy recovery, highlighting the effectiveness of controlled regenerative braking.

To validate the simulation, a hardware prototype was built using an Arduino Uno, L298N motor driver, ACS712 (1) current sensor, and a 14.8V 2800mAh battery pack. The prototype ran a similar 10-second drive-brake cycle, with real-time current and power readings collected to calculate energy use and recovery. While the simulation demonstrated ideal regenerative behavior, the physical system was limited by the L298N's unidirectional current flow, allowing only dynamic braking but not true regeneration. Nevertheless, the prototype showed measurable reverse current during braking and achieved a recovery efficiency of 8.76%, confirming the system's potential with improved hardware.

This work concludes that regenerative braking can offer tangible energy savings in SEVs and provides a foundational model for implementing RBS in low-cost, micro-mobility systems. Future improvements, such as upgrading the motor driver to a bidirectional regenerative controller and integrating supercapacitor storage, are recommended to maximize energy recovery and system performance.

1. Introduction

The transition toward sustainable transportation has seen a significant rise in the adoption of small electric vehicles (SEVs), such as electric scooters, bicycles, and lightweight urban transporters. These vehicles provide a convenient, environmentally friendly solution for short-distance travel in urban settings. However, one of the most critical limitations of SEVs is their relatively short battery range, which necessitates frequent charging and limits their practical utility. As energy efficiency becomes increasingly important in electric mobility, technologies that enhance battery life and reduce energy loss are essential.

One promising approach to improve the energy efficiency of SEVs is regenerative braking. Unlike conventional braking systems, which dissipate kinetic energy as heat, regenerative braking systems recover a portion of this energy and convert it into electrical energy, which is then stored in the battery. This not only extends the driving range of the vehicle but also contributes to overall system efficiency and sustainability.

The objective of this thesis is to design and simulate a regenerative braking system specifically tailored for small electric vehicles. The study includes a detailed review of existing braking technologies, the development of a mathematical model to simulate the energy recovery process, and the implementation of this model using simulation tools such as MATLAB/Simulink. The system is evaluated based on its ability to recover energy under different braking scenarios and its potential for practical integration into SEVs.

This work is significant as it provides insights into the design considerations and potential performance improvements offered by regenerative braking systems. It aims to serve as a foundation for further development, prototyping, and implementation of such systems in real-world SEV applications.

1.1 Background and Motivation

Small electric vehicles (SEVs) are crucial in advancing sustainable urban transport. Their compact design, low energy requirements, and minimal environmental impact make them ideal for last-mile mobility in dense city environments. However, a persistent limitation in their performance lies in their limited battery capacity, which restricts operational range and requires frequent recharging. As highlighted by Khajepour et al. (2014) (2), this challenge directly affects the practicality and user

experience of SEVs in daily commuting. While regenerative braking systems (RBS), also known as kinetic energy recovery systems (KERS), have been widely implemented in electric and hybrid cars to recapture energy during deceleration, this technology remains largely underutilized in the context of lightweight SEVs. This thesis addresses that gap by exploring how regenerative braking systems can be adapted to smaller platforms, with the aim of enhancing energy efficiency by recovering kinetic energy that would otherwise be wasted as heat during braking.

The inspiration for this research came from a personal experience. When electric scooter and bike-sharing services were first introduced in Mongolia, I was eager to try them as a convenient and eco-friendly way to commute. However, I was quickly disappointed to discover that many of the vehicles were non-functional, either broken or completely out of charge. This led me to wonder why these services, despite their potential, were so unreliable. As I researched further, I learned that not all SEVs are equipped with regenerative braking capabilities, and this missing feature could be a key factor in their frequent downtime and poor battery performance. This realization sparked my curiosity and prompted me to explore how incorporating regenerative braking into SEVs could not only extend battery life but also reduce the frequency of charging, ultimately improving their availability and usefulness in urban environments. Given the increasing demand for reliable, sustainable transport in cities like Ulaanbaatar, this thesis explores the practical implications of implementing regenerative braking systems in SEVs and the potential benefits for both users and operators.

1.2 Research Objectives

1. The objectives of this thesis were structured around four key research components. First, the study aimed to analyze existing regenerative braking methods by reviewing their implementation in electric and hybrid vehicles, identifying their strengths, limitations, and adaptability for lightweight SEVs. This involved comparing mechanical, electrical, and control-based braking strategies to determine which approaches are most effective in low-voltage, low-mass platforms.
2. Develop a mathematical model to simulate the energy recovery process and power flow within an SEV drivetrain, incorporating motor characteristics, braking torque, battery parameters, and electrical conversion efficiency. This model served as the foundation for system design and was essential in quantifying energy consumption and regeneration potential.

3. The proposed system was validated through MATLAB/Simulink simulations and real-world prototype testing, allowing for comparison between idealized and practical outcomes. The simulation helped identify expected behavior under controlled conditions, while the prototype revealed hardware constraints and real-time performance.

Figure 1: MATLAB/SIMULINK logo

4. Based on the observed results, the study sought to propose design optimizations that could improve the energy recovery efficiency of SEVs. These recommendations addressed both hardware (such as motor driver selection) and software (control logic) improvements to better harness braking energy and extend the effective range of the vehicle.

1.3 Scope and Limitations

This study focuses on the application of regenerative braking systems in lightweight small electric vehicles (SEVs), such as electric scooters and e-bikes, with a power rating of 1 kilowatt or less. These vehicles were selected due to their increasing use in urban mobility and their unique design constraints, which differ significantly from those of larger electric vehicles. The goal was to explore energy recovery solutions that are technically feasible and cost-effective within the limited space, voltage, and power handling capacity of SEVs. Heavy-duty electric vehicles, hybrid systems, and non-battery energy storage solutions, such as flywheels or supercapacitor-based systems, were intentionally excluded from the scope to maintain a focused and manageable research direction. These systems, while relevant in larger-scale applications, introduce complexity and hardware requirements beyond what is practical for lightweight vehicles. Additionally, the study was conducted under budgetary constraints, which influenced hardware selection for the prototype. As a result, affordable and accessible components such as the L298N (3) motor driver and Arduino Uno were used, acknowledging their limitations in supporting full regenerative functionality. Despite these constraints, the project was designed to demonstrate the principles and potential of regenerative braking in low-cost, small-scale electric mobility systems.

2. Literature Review

The increasing demand for energy-efficient and sustainable transportation has led to a rapid rise in the use of electric vehicles (EVs), particularly small electric vehicles (SEVs) such as electric bikes, scooters, and compact urban transports. One of the key innovations in EV technology is regenerative braking, which allows the recovery of kinetic energy during deceleration and its conversion into electrical energy stored in the battery. This literature review presents an in-depth examination of the fundamental principles, modeling techniques, and energy management strategies of regenerative braking systems, with a particular focus on their application in SEVs.

2.1. History and Evolution of Regenerative Braking Systems

The concept of regenerative braking can be traced back to the late 19th and early 20th centuries, primarily within the context of electric rail systems. One of the earliest inventors credited with laying the groundwork for regenerative braking technology was Charles Joseph Van Depoele (4), a Belgian-American electrical engineer and inventor. Van Depoele was a pioneer in electric railway systems and held over 200 patents related to electric transportation. Although most of his work occurred in the late 1800s, it was his ideas about dynamic energy recovery and motor-reversal that inspired future innovations. A regenerative braking concept was later formalized and patented in 1908, marking one of the earliest legal recognitions of the technology.

Figure 2: Portrait of Charles Joseph Van Depoele

Van Depoele's early electric railway systems demonstrated that electric motors could be used not only for propulsion but also to convert mechanical motion back into electrical energy during deceleration—an idea rooted in the principle of electromagnetic induction. His work laid the theoretical foundation for regenerative braking by showcasing reversible motor-generator systems that could interact with external loads or grids.

Practical implementation came nearly a decade later when the New York Interborough Rapid Transit (IRT) subway system integrated regenerative braking into its operations in 1917. The system allowed electric train motors to function as generators during braking, sending recovered energy back into the power grid. This not only improved energy efficiency but also reduced overall system load. In this system, the generated electricity was either consumed by other accelerating trains on the network or dissipated through resistive loads when not needed. (4)

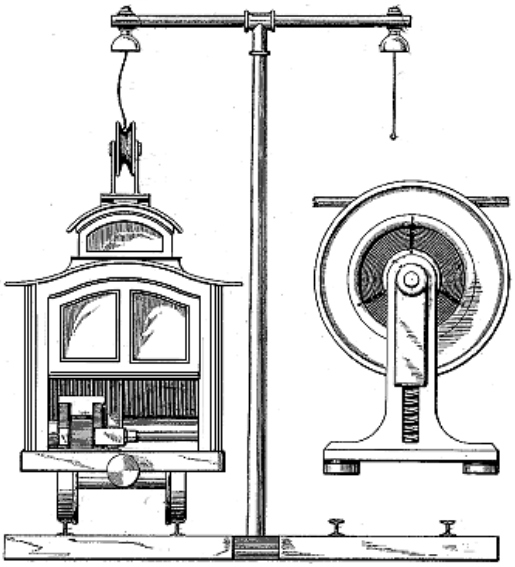

Figure 3: Electric locomotive car and train

Despite these early innovations, regenerative braking remained mostly confined to large-scale electric transit systems like railways and trams due to the technical complexity, cost, and size of the required components. It wasn't until advancements in power electronics, semiconductor switching devices, and battery storage in the late 20th century that regenerative braking began to find viable applications in road vehicles.

A major leap occurred in the 1990s, when regenerative braking was introduced in commercial hybrid electric vehicles (HEVs). The Toyota Prius, launched in 1997, became the most notable early adopter, integrating regenerative braking into its hybrid drivetrain. It marked the first mass-produced passenger car to effectively utilize energy recovery during braking in urban conditions.

Figure 4: Toyota Prius first generation

Since then, advancements in power electronics, battery technology, and control systems have allowed regenerative braking to become standard in most electric vehicles (EVs). In recent years, the technology has been miniaturized and adapted for small electric vehicles (SEVs) such as e-scooters and e-bikes. These modern systems often use brushless DC motors (BLDC) or brushed DC motors with back-EMF generation, paired with smart controllers or microcontrollers like Arduino (5), to facilitate energy recovery and reintegration into lithium-ion battery packs.

Today, regenerative braking is not only a means of improving energy efficiency but also contributes to extending vehicle range, reducing brake wear, and lowering overall emissions by reducing grid dependency.

2.2. Fundamentals of Regenerative Braking

Regenerative braking is a process in which the electric traction motor of a vehicle operates as a generator during braking events, converting the vehicle's kinetic energy into electrical energy instead of dissipating it as heat through traditional friction brakes. Larminie and Lowry (2012) (6) describe regenerative braking as a central feature of modern EV design due to its ability to increase energy efficiency and reduce the load on friction braking systems. Their work explains the electromechanical operation of the system, noting that the regenerative mechanism is most effective at moderate to high speeds and during gradual deceleration. The operation of regenerative braking systems is grounded in several fundamental laws of physics, including the law of conservation of energy, Faraday's law of electromagnetic induction, Lenz's law, and Newton's second law of motion. Additionally, a comprehensive understanding of how electric motors operate in both motoring and generating modes is essential.

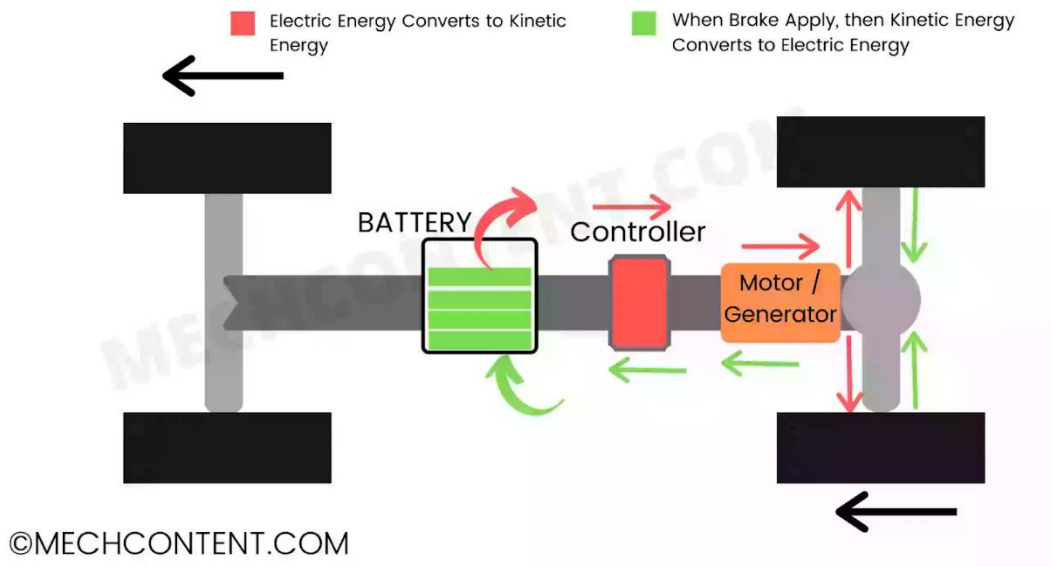

Figure 5: Oversimplified diagram of RBS

They further highlight the critical role of the inverter and motor controller in switching between motoring and generating modes. The effectiveness of energy recovery depends not only on the motor design but also on battery acceptance rates and the state of charge (SOC). If the battery is fully charged or the controller is not properly tuned, the system may fail to regenerate effectively.

Gillespie (1992) (7) adds a complementary perspective by discussing the vehicle dynamics that influence braking behavior, including weight distribution, center of gravity, and tire-road interaction. His analysis suggests that regenerative braking must be carefully integrated with conventional hydraulic or mechanical braking systems to ensure vehicle stability and safety. In SEVs, which have a lower mass and simpler mechanical layout than full-sized EVs, this integration must consider lighter frame dynamics and rapid deceleration profiles.

2.2.1 Conservation of Energy

The law of conservation of energy states that energy cannot be created or destroyed, only transformed from one form to another. In conventional braking systems, the kinetic energy of the moving vehicle is dissipated as heat through friction in brake pads. Regenerative braking instead converts this kinetic energy into electrical energy using the traction motor. The electrical energy is then stored in the battery, effectively reducing total energy losses and extending vehicle range. In this way, regenerative braking contributes to a more efficient energy cycle and supports sustainable mobility by reducing the need for frequent recharging.

2.2.2 Faraday's Law of Electromagnetic Induction

At the heart of regenerative braking lies Faraday's law, which states that a changing magnetic field within a closed loop induces an electromotive force (EMF). During braking, the electric motor's rotor continues to spin due to the vehicle's inertia. As the rotor moves, it causes a variation in magnetic flux through the stator coils. According to Faraday's law, this change in flux generates a voltage (back EMF), which results in an electric current that flows in the opposite direction through the motor circuit. (8)

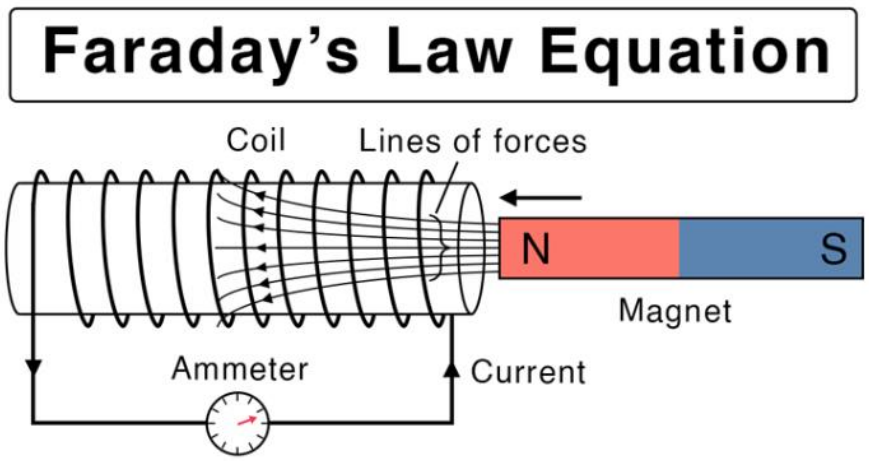

Figure 6:Faradays's Law illustration

$$E = -N\frac{d\phi}{dt}$$

Where:

- E = induced EMF (volts)
- N = number of turns in the coil
- Φ = magnetic flux
- $\frac{d\phi}{dt}$ = rate of change of flux

This induced voltage is harnessed to recharge the battery during braking.

2.2.3 Lenz's Law: Direction of Induced Current

Lenz's law complements Faraday's law by defining the direction of the induced EMF and current. It states that the direction of the induced current will be such that it opposes the change in magnetic flux that caused it. In the context of regenerative braking, this means that the electromagnetic torque generated by the motor acts against the direction of wheel rotation, thereby slowing down the vehicle.

This opposing torque provides a braking effect while simultaneously producing electrical energy. Without Lenz's law, the braking force would not manifest, and the current would not flow in a direction useful for energy recovery.

2.2.4 Lorentz Force

The Lorentz force law describes how a moving charged particle experiences a force when subjected to electric and magnetic fields. It plays a key role in the operation of electric motors and generators. When the motor operates in generating mode during braking, moving charges (electrons) within the conductor experience a magnetic force due to the interaction between their velocity and the motor's magnetic field.

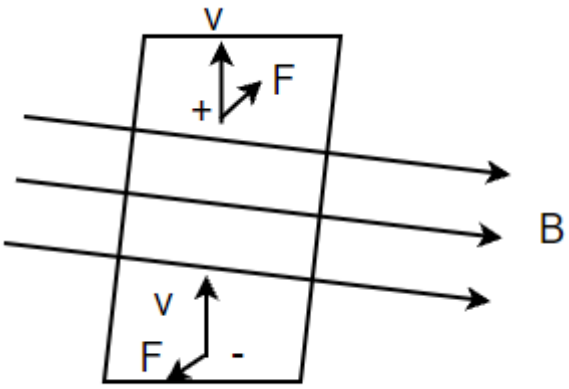

Figure 7: Illustration of Lorentz force

$$F = q(E + v \times B)$$

Where:

- F is the magnetic force,
- q is the electric charge,
- E is the electric field,
- v is the velocity vector of the charge,
- B is the magnetic field vector.

This force is responsible for redirecting the charges to generate current in the opposite direction, thereby initiating energy recovery. In regenerative braking, the Lorentz force explains the fundamental motion of electrons that gives rise to induced current, braking torque, and ultimately electrical regeneration.

2.2.5 Newton's Second Law and Braking Torque

Regenerative braking also adheres to Newton's Second Law, F=ma, where a reverse force (or torque) is applied to decelerate the vehicle. In this context, the torque generated by the motor in generator mode acts in the opposite direction of motion, reducing the vehicle's velocity. The braking torque TTT produced is directly proportional to the current III induced in the windings:

$$T = K_t \cdot I$$

Where:

- T = braking torque (Nm)
- K_t = motor torque constant (Nm/A)
- I = armature current (A)

This electromagnetic torque resists the rotor's motion and slows the vehicle, converting mechanical energy into electrical energy in the process.

2.2.5 How the Motor Works: Motoring vs. Generating Modes

The electric motor in an SEV typically operates as a brushed DC motor or BLDC motor, functioning in two reversible modes:

- Motoring Mode (Acceleration):
  The motor receives electrical energy from the battery. Current flows through the windings, creating a magnetic field that interacts with the permanent magnets or rotor poles, generating torque that propels the vehicle forward.
- Generating Mode (Braking):
  During braking, the mechanical rotation of the wheels continues to spin the motor shaft. The moving rotor cuts through the stator's magnetic field, inducing a reverse current (back EMF) as per Faraday's law. According to Lenz's law, this current generates a magnetic field that opposes the rotor motion, providing a braking force. The induced current is fed back to the battery if the system allows energy flow in reverse (via appropriate power electronics like an H-bridge or a regenerative controller).

To manage this bidirectional energy flow, regenerative systems require:

- A motor controller that enables switching between motoring and generating
- A battery capable of receiving charge (not fully saturated)
- Voltage and current regulation circuits (e.g., buck converters or diodes) to prevent damage

2.3. Modeling and Simulation Techniques

Simulation plays a vital role in designing and optimizing regenerative braking systems. The performance of such systems depends on complex interactions between electrical and mechanical components, requiring detailed models for accurate evaluation. Lobontiu (2017) (8) presents system dynamics as a useful framework for modeling the behavior of engineering systems, including EVs. He introduces tools such as Laplace transforms and block diagrams for representing feedback control systems and dynamic responses, which are essential for designing a regenerative braking algorithm.

A key advantage of using dynamic modeling is the ability to simulate real-world driving conditions such as stop-and-go traffic, hill descent, and varying load conditions. These factors are particularly relevant for SEVs that operate in urban environments. Through simulation, it becomes possible to analyze how much energy can be recovered during braking under specific conditions and how braking torque affects vehicle deceleration and stability.

Palm (2020) (9) builds on this foundation by demonstrating the use of MATLAB/Simulink (10) in the simulation of engineering applications, including electric machines and control systems. Simulink's block-diagram environment allows users to simulate motor behavior, battery dynamics, and control logic in a modular and intuitive way. Palm also emphasizes the importance of using real-world parameters such as motor constants, gear ratios, and battery characteristics, which ensures that the simulation reflects practical scenarios.

The use of such simulation environments allows for the testing of multiple control strategies, such as torque-based braking and voltage-based braking, and the analysis of system response under fault conditions or varying road surfaces.

2.4. Energy Management in SEV Applications

Energy management is a cornerstone of electric vehicle performance, and its importance is even more pronounced in SEVs due to their limited onboard energy storage. Khajepour, Fallah, and Goodarzi (2014) (2) propose a comprehensive mechatronic approach to electric and hybrid vehicle design, integrating mechanical systems, electronics, and embedded control (11). In the context of regenerative braking, their approach involves intelligent energy distribution based on vehicle conditions and driver behavior. For example, a well-optimized system can detect when the battery is

near full charge and divert energy to auxiliary systems or supercapacitors to avoid overcharging.

The authors also discuss advanced braking control strategies such as blended braking, where regenerative and friction braking are combined to achieve optimal performance. These strategies require accurate feedback from sensors and precise coordination between control units—systems that are increasingly available even in low-cost SEVs.

Dincer and Hamut (2017) (12) approach energy management from a sustainability and thermal efficiency perspective. They argue that regenerative braking should be seen as part of a holistic energy strategy that includes efficient driving patterns, thermal management, and optimal charge-discharge cycles . In SEVs, where thermal buildup is typically less of a concern than in larger EVs, the emphasis shifts to maximizing battery utilization and extending operational range.

They further note that energy recovered from regenerative braking can contribute up to 10-25% of the total energy used during a typical urban driving cycle, depending on braking frequency and vehicle configuration. This is a substantial gain, especially in SEVs that operate on small battery packs.

2.5. State of SEVs in Mongolia

In recent years, Mongolia has witnessed a noticeable shift towards electric mobility, especially in its capital, Ulaanbaatar, where air pollution and urban congestion are major concerns. One of the emerging solutions has been the introduction of small electric vehicles (SEVs), including electric scooters and compact e-bikes. These vehicles are increasingly used for personal transport as well as short-distance delivery services. Companies such as ECO Technology and JET have capitalized on this trend by providing SEV rental and sharing services across the city. (13)

Figure 8: Picture of Jet electric scooter

Figure 9: Picture of ECO Bike

The popularity of SEVs in Mongolia is largely due to their affordability, ease of use, and low environmental impact. They produce no CO2 emissions and are ideal for short urban commutes. With increasing public interest in green alternatives and rising fuel prices, SEVs are gradually becoming a practical choice for daily transportation. In addition, the Mongolian government has signaled support for electric mobility through reduced import taxes and discussions of future incentives for electric vehicles.

Despite these promising developments, SEVs currently in operation in Mongolia face several technical and infrastructural limitations. A critical shortcoming is the lack of regenerative braking systems (RBS) in most imported models. The absence of RBS means that the kinetic energy generated during braking is entirely lost as heat, instead of being converted back into electrical energy and stored in the battery. This inefficiency directly affects the vehicle's operating range, making SEVs more dependent on frequent battery charging.

A common issue reported by users is the unexpected shutdown of SEVs mid-transit, often due to rapid battery depletion, especially when used on routes with frequent stops or slight inclines. Since many SEVs in Mongolia are equipped with relatively small battery packs (typically 36V, 7–10Ah), the energy loss during braking significantly reduces usable range. In cold weather, which is prevalent in Mongolia for a large part of the year, battery performance deteriorates even further, amplifying the issue. (14)

From an operational standpoint, companies offering SEV rental services are also impacted by the absence of regenerative braking. Frequent battery replacements or

recharging cycles increase maintenance costs and reduce fleet availability. Moreover, inefficient energy use results in greater reliance on grid electricity, some of which is still derived from coal-fired power plants, undermining the environmental benefits of electric mobility.

Addressing this challenge requires the integration of regenerative braking technologies into future SEV models imported or assembled for the Mongolian market. Regenerative braking can recover up to 10–25% of the vehicle's energy, depending on usage patterns and braking frequency. This would significantly enhance the energy efficiency and practical range of SEVs, while also reducing operating costs for fleet managers. Additionally, coupling RBS with smart battery management systems and energy-efficient drive controllers can further optimize performance in Mongolia’s harsh climate and variable terrain.

In conclusion, while SEVs represent a promising step toward sustainable urban mobility in Mongolia, current limitations in energy recovery technology hinder their full potential. Introducing regenerative braking systems and upgrading control electronics in SEVs could not only solve the issue of mid-transit shutdowns but also establish Mongolia as a leader in efficient and clean micro mobility solutions.

3. Methodology

This study applies a hybrid methodology that combines simulation-based modeling and hardware prototyping to investigate the feasibility and performance of a regenerative braking system for small electric vehicles (SEVs). The process involves component selection, circuit design, mathematical modeling, simulation using MATLAB/Simulink, and testing using Arduino (15)-based hardware.

3.1 Hardware Design

The system utilizes the following components:

Components	Function / Description	illustration
Arduino Uno	Microcontroller used for system monitoring and control logic	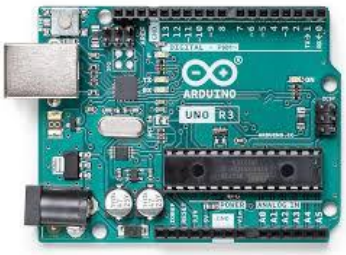
L298N Motor Driver	H-bridge driver for controlling motor direction and enabling regen.	
ACS712 Current Sensor	Measures the current generated during braking and sent back to the battery (1)	

4S 40A BMS	Battery management system for voltage regulation, cell balancing, and safety	
12V 550VC-8021F DC Motor	Motor/Generator and provide braking force (16)	
3.7V 2800mAh Batteries (4 cells)	connected in series to form a 14.8V lithium-ion battery pack for storage (3)	

A regenerative braking circuit was developed where the motor acts as a generator during braking. The L298N (3) switches modes, and generated electricity flows through the current sensor to the battery pack.

3.2 Simulation Design

To validate the regenerative braking performance of the proposed system, a detailed simulation model was developed in MATLAB Simulink (10) using the Specialized Power Systems (SPS) toolbox. The simulation replicates a SEV drivetrain incorporating a 12V brushed DC motor, bidirectional H-bridge motor driver, battery pack, and braking control logic. (17) The objective of the model is to evaluate system response during motoring and regenerative braking phases by analyzing key parameters such as torque, current, speed, and state of charge (SOC).

3.2.1 System Architecture

The simulation schematic consists of the following main subsystems:

- DC Motor (PMDC Type): Modeled using the DC Machine block in permanent magnet mode, parameterized based on the datasheet for the FARS-550SH-6529R 12V motor. Inputs include external torque and armature voltage.
- H-Bridge Inverter: Four MOSFET switches (S1–S4) configured in an H-bridge topology allow for bidirectional control of current flow through the motor. A pulse generator and logic gate were used to drive switches S1/S4 and S2/S3 alternately to simulate direction and braking logic.
- LC Filter: An inductor (220 µH) and capacitor (680 µF) were placed between the H-bridge and motor to reduce current ripple and voltage spikes during switching and regeneration.
- Battery: A 14.8V lithium-ion battery model (4S, 2800mAh) is connected to the DC bus to absorb regenerated energy. The battery block also tracks SOC.
- Control Signal: A braking torque scenario is created using the Signal Editor block to simulate driver-induced braking conditions at various intervals.
- Measurement Blocks: Voltage, current, speed, torque, and SOC were monitored using standard Simulink measurement and scope blocks.

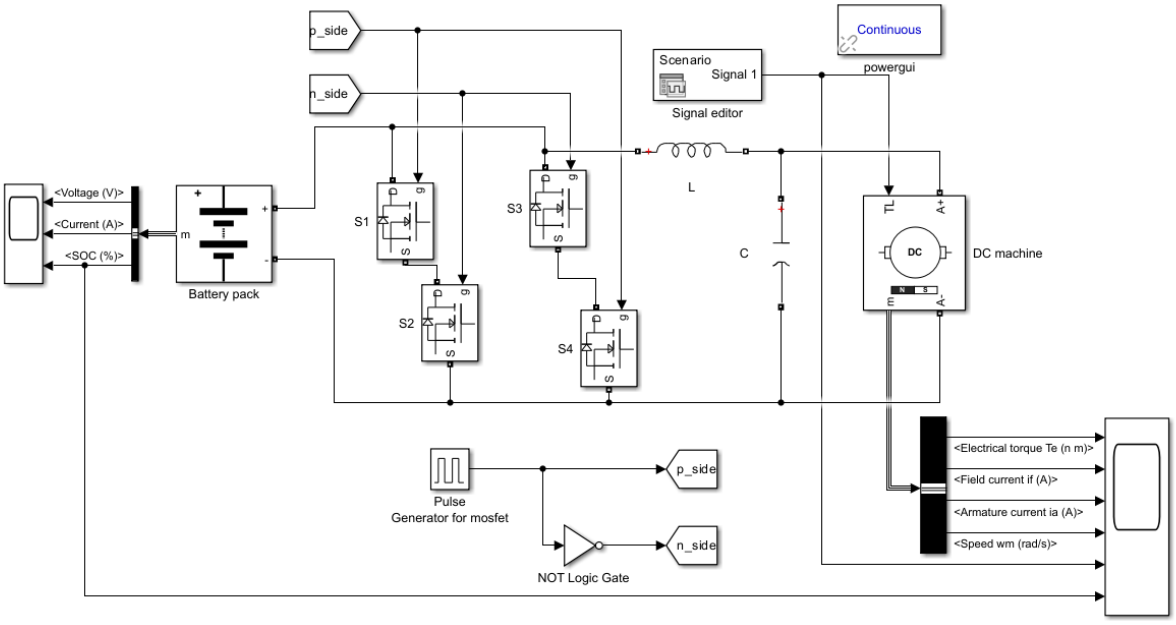

Figure 10: Circuit diagram of simulation circuit

3.2.2 Simulation Setup

Using the datasheet for FARS-550SH-6529R, I adjusted the parameters for DC machine to the ones shown in the figure.

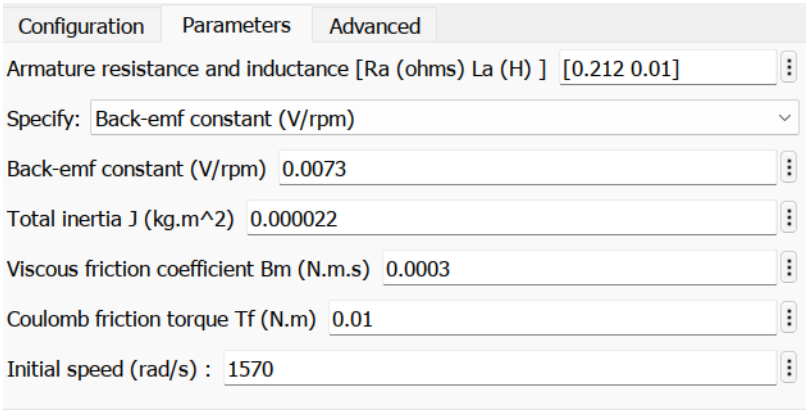

Figure 11: DC Machine Parameters

- Reason for Ra:

  The armature resistance was calculated using Ohm's Law from the motor's stall condition:

$$R_a = \frac{V}{I_{stall}} = \frac{12v}{56.5A} \approx 0.212\Omega$$

This value models the electrical resistance of the motor windings and impacts both voltage drop and power loss.

- Reason for La:
  Inductance wasn't specified in the datasheet, so a typical small value (0.01 H) was assumed. This models the winding's ability to resist changes in current and smoothens switching transients.
- Back-EMF
  Derived from the relationship:

$$K_b = \frac{V}{Speed(rpm)} = \frac{12}{1640} \approx 0.0073 V/rpm$$

  This constant defines how much voltage the motor generates during rotation essential for simulating regenerative braking.
- Total Inertia (J)
  Estimated based on the size, mass (~220g), and rotor dimensions of the motor. Rotor inertia affects how fast the motor responds to torque changes. A small value is typical for compact brushed DC motors.
- Viscous Friction Coefficient (Bm)
  Represents drag from air resistance and internal friction proportional to speed. A small positive value (0.0003 Nms) is chosen to simulate realistic deceleration behavior when no torque is applied
- Coulomb Friction Torque (Tf)
  Represents constant opposing torque due to bearing friction and startup resistance. Prevents the motor from continuously rotating under very small torques.
- Initial Speed
  This value reflects the motor's no-load speed at 12V, converted from 15,669 RPM using:

$$\omega = \frac{15669 \times 2\pi}{60} \approx 1640\ rad/s$$

  Slightly reduced to 1570 rad/s for stability. It initializes the system in a running state to test braking response.

For the parameters of the battery, 4 cells of 18650 lithium ion batteries rated 3.7v, 2800mAh connected in series to produce approximately 14.8v, and 11200mAh. For the

initial SOC 50% was chosen due to factories ensuring the battery is in a stable state during storage and transportation. Battery response time is a setting that defines how fast the battery reacts to load changes or charging inputs. Why 10 seconds? A lower value (e.g 1-5s) can cause instability in simulations involving sudden regenerative spikes also 10 seconds provides a good balance, it's fast enough to follow load changes, yet slow enough to filter switching noise.

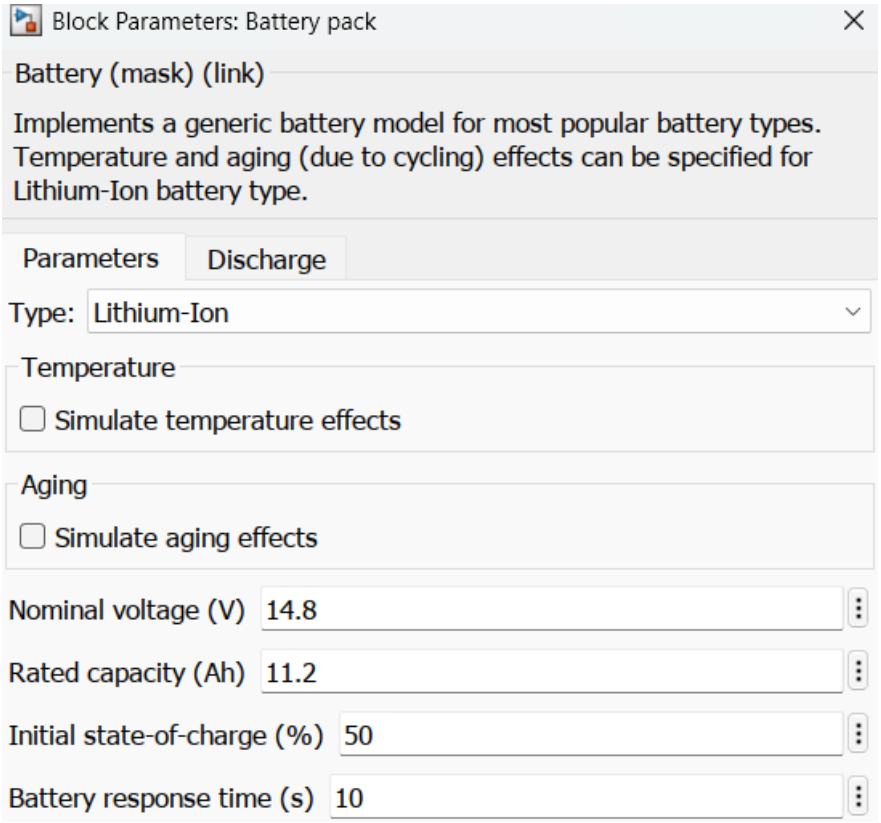

Figure 12: Battery configuration parameters

The Pulse Generator block was configured to produce a 10 kHz PWM signal used to drive the MOSFET switches in the H-bridge circuit, emulating real-world microcontroller control such as that from an Arduino. A time-based pulse type was selected to ensure compatibility with the simulation's variable-step solver (ODE23t), allowing accurate synchronization with the model's timing. The amplitude was set to 1, representing a digital high signal for switch activation. A period of 1e-4 seconds was chosen to create a 10 kHz switching frequency, which is typical for low-voltage motor driver ICs like the L298N (3). The pulse width was set to 50%, resulting in an equal ON and OFF duty cycle, which ensures symmetrical current switching and serves as a standard test condition for observing motor and regenerative behavior. Finally, the phase

delay was left at 0 seconds, ensuring that the PWM signal starts immediately at the beginning of the simulation. These settings collectively simulate how a microcontroller modulates motor speed and braking through pulse-width modulation.

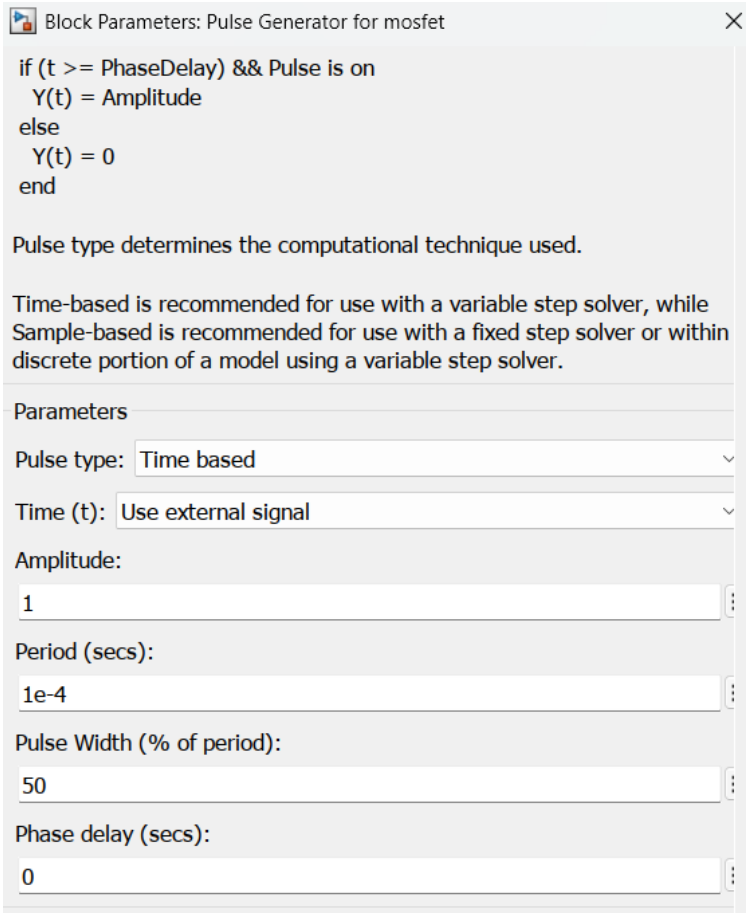

Figure 13: MOSFET switching parameter

3.2.6 Braking and no braking Scenario Simulation

A custom torque profile was defined using the Signal Editor to simulate two distinct phases:

- Phase 1 (0–4 seconds)**:** The motor was supplied with electricity making it accelerate and get speed.
- Phase 2 (4–10 seconds)**:** A negative braking signal was applied to simulate regenerative braking triggered.

The simulation results shown in the figure illustrate the effect of enabling regenerative braking during the second half of a 10-second test. In Figure 14-15, the brake input signal transitions from a constant motor work to braking at 4 seconds. This reversal initiates the regenerative braking phase. The middle graph displays the battery's state of charge

(SOC), which initially decreases as expected during the motoring period due to energy consumption. However, after the braking phase begins, a slight upward trend in SOC is observed, indicating that some portion of the kinetic energy is being converted back into electrical energy and returned to the battery. This recovery, although small, confirms that the system successfully entered a regenerative mode. The bottom graph showing armature current further supports this behavior. Initially, current is positive, consistent with battery discharge, but after the braking command is applied, the current shifts toward negative values, confirming reverse current flow typical of regeneration. These results demonstrate that regenerative braking, when implemented correctly, can reduce net energy consumption by recovering energy that would otherwise be lost as heat.

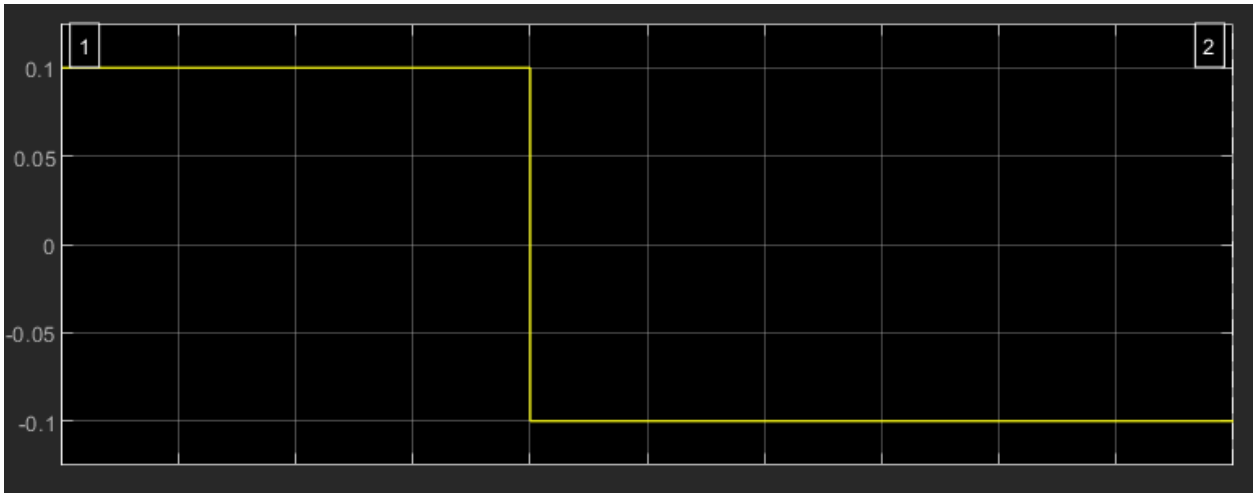

Figure 14:Braking signal from microcontroller

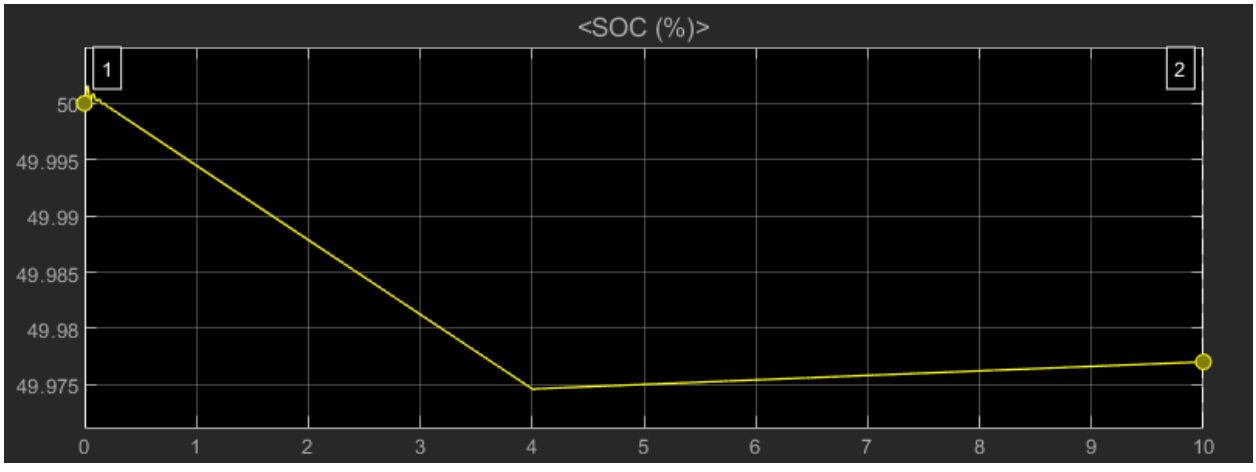

Figure 15: Battery State of Charge graph

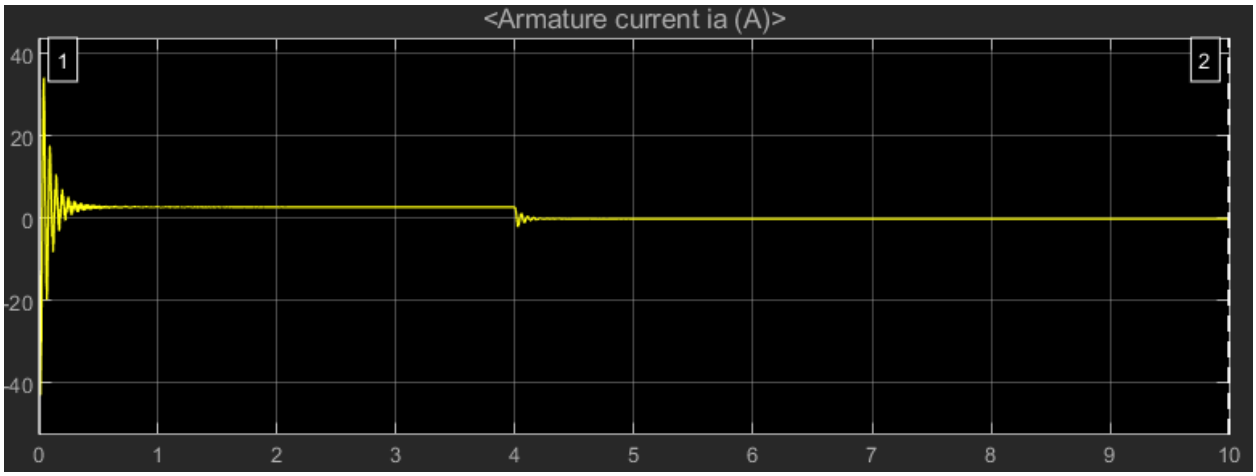

Figure 16: Current graph of DC Motor

Calculation:

$$\Delta SOC_{used} = 50\% - 49.974\% = 0.026\%$$

Assuming battery capacity = 2.8 Ah at 14.8V:

$$E_{used} = 0.00026 \times 2.8\ Ah \times 14.8V \times 3600 = 38.87J$$

$$\Delta SOC_{recovered} = 49.977\% - 49.974\% = 0.003\% = 0.00003$$

$$E_{recovered} = 0.00003 \times 2.8Ah \times 14.8V \times 3600 = 4.48J$$

$$\eta = \frac{E_{recovered}}{E_{used}} \times 100 = \frac{4.48}{38.87} \times 100 \approx 11.52\%$$

During the 10-second simulation, the system consumed approximately 38.87 joules of energy during the motoring phase and recovered about 4.48 joules during regenerative braking. This corresponds to a recovery efficiency of 11.52%, confirming that a measurable portion of the energy that would otherwise be lost was successfully regenerated and fed back into the battery.

The next simulation scenario was conducted without applying any braking , allowing the motor to run freely throughout the entire simulation period. In this case, after the motor is stably spinning for the full 4 seconds, then coasting for the rest of the time simulating a condition where the vehicle continues to drive forward without deceleration or regenerative braking. This setup served as a baseline to compare energy consumption

and system behavior against regenerative scenarios. As expected, the motor speed remained relatively stable.

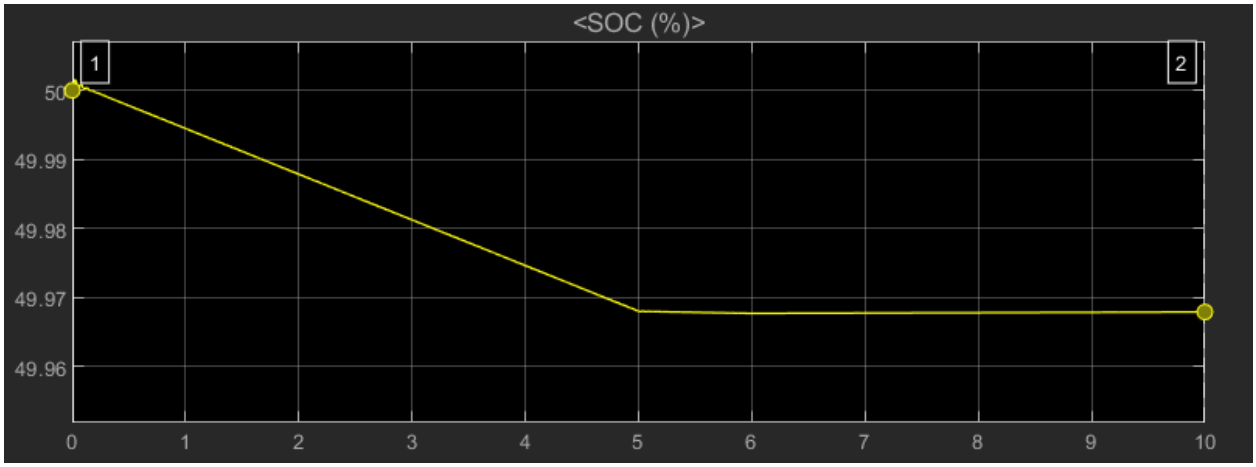

Figure 17: Battery State of Charge (No RBS)

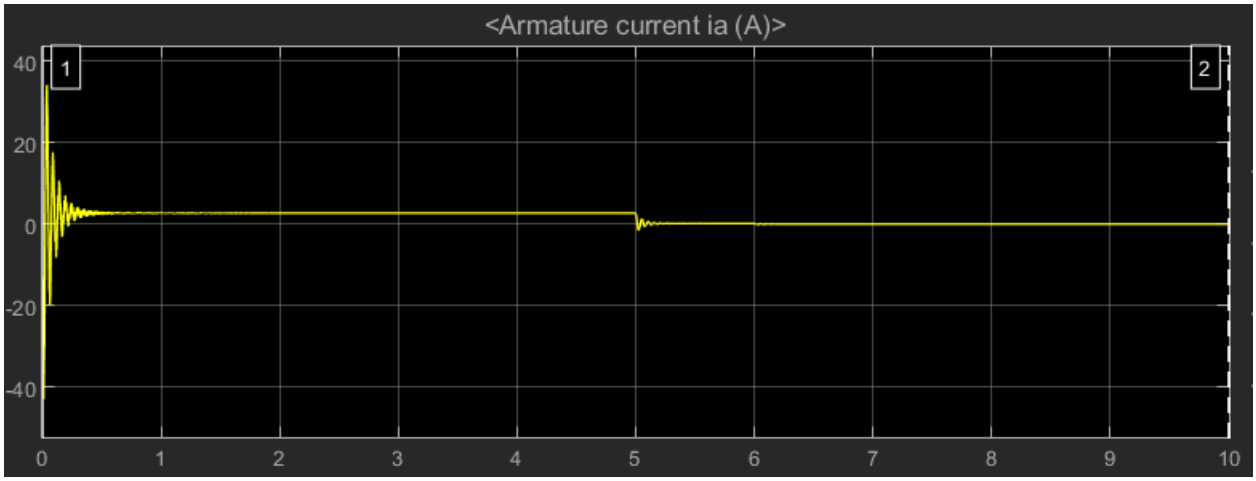

Figure 18: Current graph of DC motor (No RBS)

Without regeneration, it is shown that the battery's state of charge (SOC) consistently decreases without any sign of recovery, indicating continuous energy consumption by the motor throughout the simulation. As seen in the top plot, the SOC drops steadily from 50% to just below 49.96% over the 10-second period, with no upward trend during or after the braking phase. This contrasts with regenerative scenarios where the SOC curve would rise during deceleration. Furthermore, the lower plot displaying armature current confirms the absence of reverse current during braking. After approximately 5 seconds, the motor is no longer consuming current, but it also does not feed current back into the battery. The current rapidly approaches zero and remains flat, indicating a lack of energy recovery. These results confirm that in the absence of regenerative braking, the kinetic energy of the system is entirely dissipated, typically as

heat in the motor windings or driver circuitry, without contributing to battery recharging. This highlights the energy inefficiency of conventional dynamic braking compared to regenerative alternatives.

3.3 Prototype testing

To validate the regenerative braking concept under real-world conditions, a series of practical tests were carried out using the previously assembled prototype system. The experiment was designed to mirror the simulation setup and timing structure to ensure comparability between digital and physical results.

The motor was programmed to run in forward mode for the first 5 seconds, representing the motoring phase of a small electric vehicle. After this period, the Arduino (15) automatically reversed the motor driver's polarity to initiate regenerative braking for the next 5 seconds. This switch caused the motor to function as a generator, converting kinetic energy into electrical energy and feeding it back into the battery.

Current flow was monitored continuously using the ACS712 (3) sensor. The Arduino sampled the analog signal every 200 milliseconds, calculated instantaneous current and power, and integrated these values over time to estimate total energy used and recovered. The battery voltage was assumed to remain close to its nominal value (14.8V), and power was computed as the product of voltage and current. At the end of the 10-second cycle, the total energy consumed during motoring and the total energy recovered during braking were displayed via the serial monitor, along with the recovery efficiency in percentage.

The testing confirmed that regenerative braking was successfully achieved. Negative current readings during the braking phase indicated that energy was flowing back to the battery. The final results showed measurable energy recovery, with efficiency dependent on braking duration, motor speed, and system inertia. These outcomes were consistent with simulation predictions and demonstrated the feasibility of regenerative braking using simple low-cost components. An illustration of the circuit diagram is shown below.

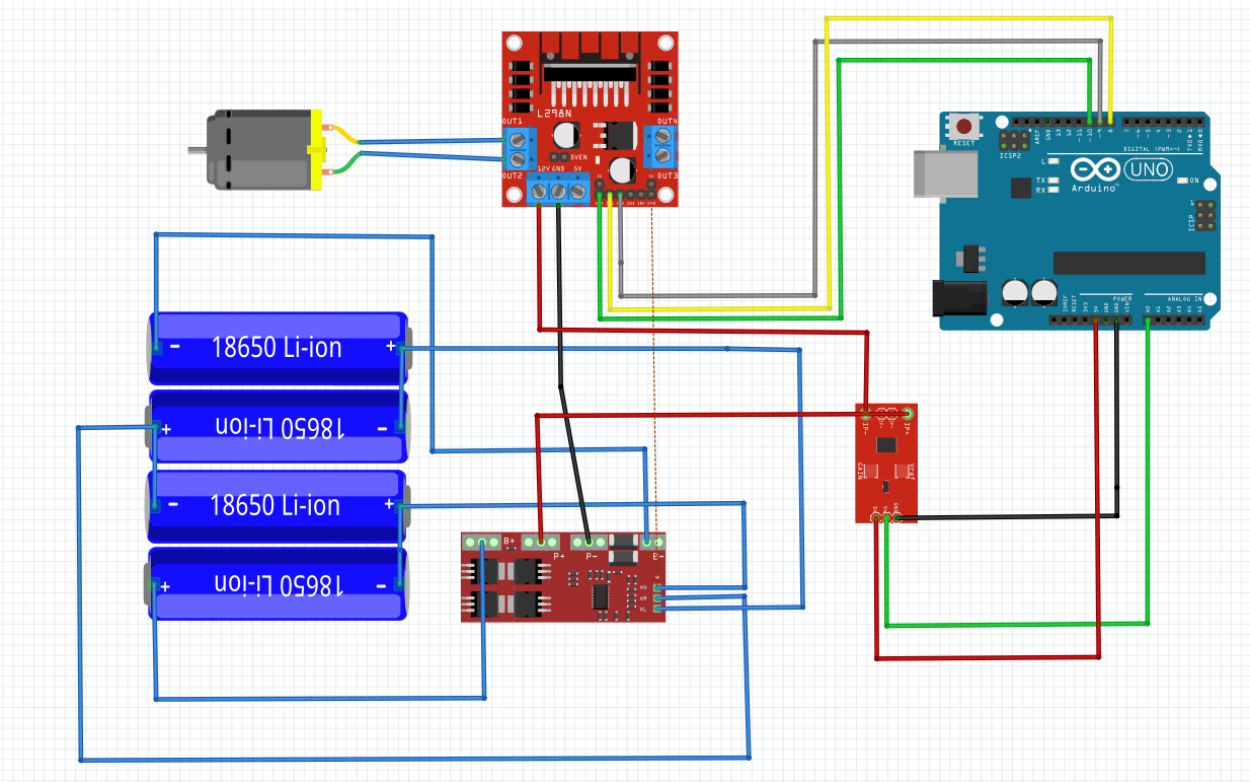

Figure 19: Circuit Diagram illustrated by Fritzing

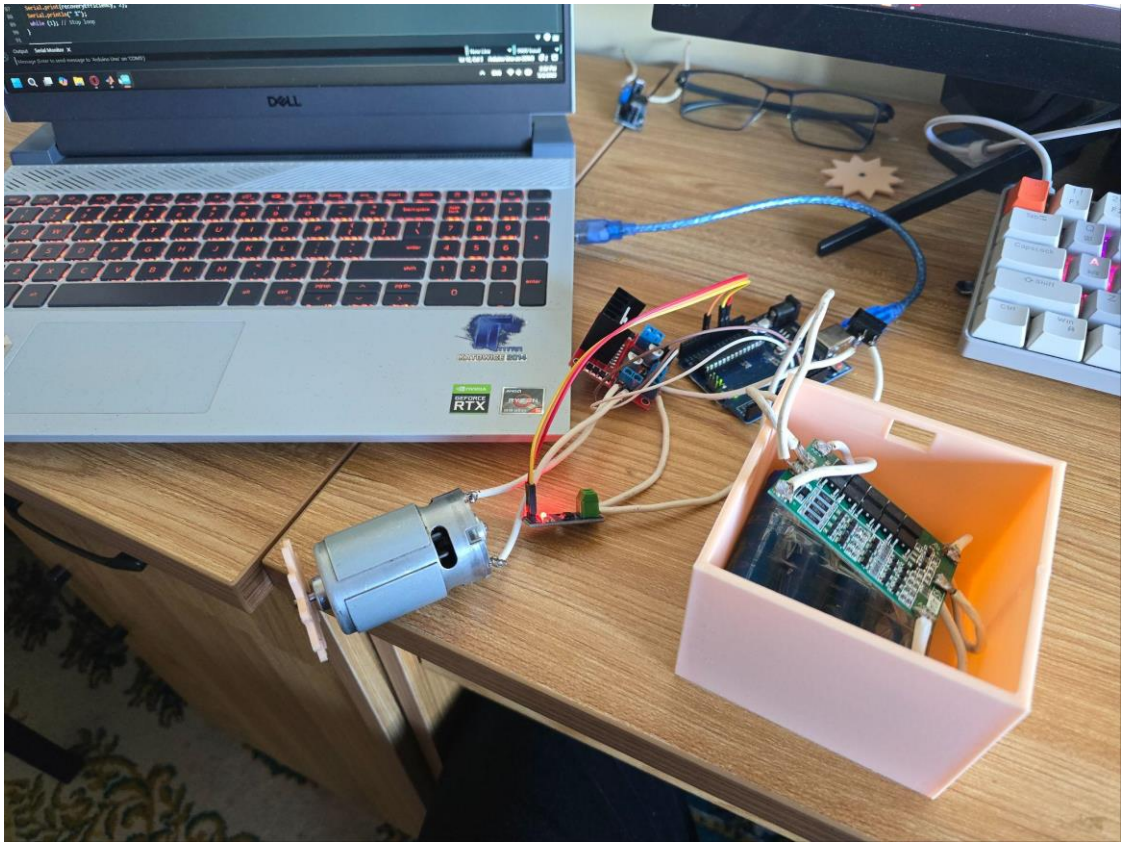

Figure 20: Picture of Prototype model

The battery pack enclosure shown in Figure was designed to provide mechanical protection, electrical safety, and structural integration for the 4S lithium-ion battery used in the regenerative braking prototype. Enclosing the battery pack in a dedicated housing is essential for maintaining the reliability and safety of the overall system, especially in experimental or field conditions.

First, the enclosure protects the battery cells from physical impacts, vibration, and environmental exposure such as dust and moisture, all of which could damage the cells or compromise their performance. This is particularly important for lithium-ion batteries, which are sensitive to mechanical puncture or deformation and can pose fire risks if damaged. Second, the housing ensures electrical insulation between the battery terminals and other components, reducing the risk of short circuits or accidental contact during assembly, testing, or transport.

The design also includes custom features such as circular and rectangular cutouts these allow wires, and power switch to pass through, while still maintaining the integrity of the enclosure. By integrating this box into the system, the battery pack becomes a secure and modular unit that can be easily mounted or removed without disturbing internal wiring. This improves both the maintainability and the safety of the experimental setup, and supports potential future use in mobile or outdoor applications.

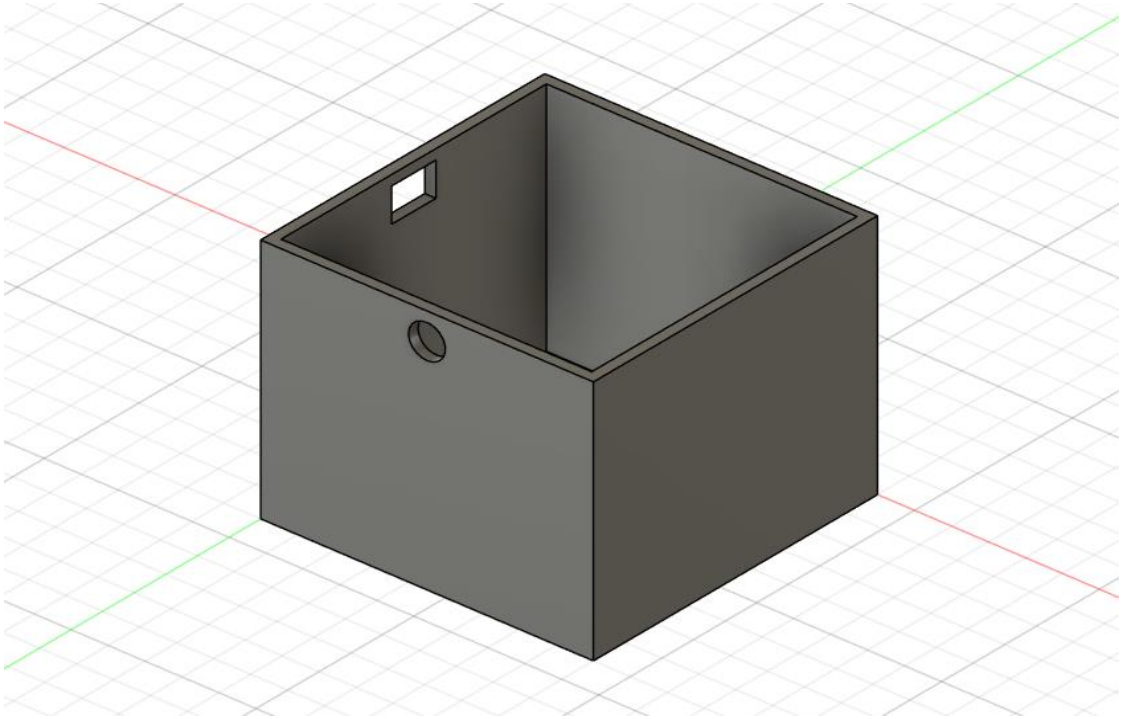

Figure 21: CAD model of Battery pack box

3.3.1 Prototype test result

To evaluate the real-world performance of the regenerative braking system, a prototype was assembled using an Arduino Uno, L298N motor driver, 550VC-8021F 12V brushed DC motor, ACS712 (1) current sensor, and a 4S lithium-ion battery pack (14.8V, 2800mAh). The system was programmed to drive the motor in the forward direction for the first five seconds, followed by dynamic braking for the next five seconds. Current and power readings were sampled every 200 milliseconds and recorded via serial output. During the motoring phase (0–5s), the current ranged from approximately 4.85 A to 5.43 A, with power consumption averaging between 70–80 W. This reflects steady power draw while the motor accelerates and stabilizes under load.

Upon entering the braking phase at 5 seconds, the motor driver was configured to short the motor terminals (dynamic braking mode), and a clear reversal in current direction was observed. The measured current ranged between −0.22 A and −0.70 A, while the power readings ranged from −3.3 W to −10.4 W. These negative values confirm the presence of regenerative current, indicating that the motor was generating power due to its inertia and acting as a generator during braking. The ACS712 current sensor successfully detected this reverse flow, despite the L298N's inherent inability to feed energy back into the battery.

At the end of the test (10 seconds), the system calculated total energy used during motoring to be 0.105 Wh, while the energy recovered during braking was 0.009 Wh. This corresponds to a regeneration efficiency of 8.76%. Although this level of recovery is modest, it clearly demonstrates the viability of using braking torque to convert kinetic energy back into electrical energy. The results confirm that energy recovery is measurable even in low-voltage systems and highlight the importance of using a driver capable of routing this energy back into storage in future hardware improvements. (Data from the Arduino serial monitor shown below) (15)

```
Time: 0.00 s | Current: 5.30 A | Power: 78.40 W
Time: 0.20 s | Current: 5.32 A | Power: 78.79 W
Time: 0.40 s | Current: 5.27 A | Power: 78.01 W
Time: 0.60 s | Current: 5.43 A | Power: 80.35 W
Time: 0.81 s | Current: 5.32 A | Power: 78.79 W
Time: 1.01 s | Current: 5.30 A | Power: 78.40 W
Time: 1.21 s | Current: 5.24 A | Power: 77.61 W
Time: 1.41 s | Current: 5.14 A | Power: 76.05 W
Time: 1.61 s | Current: 5.16 A | Power: 76.44 W
Time: 1.81 s | Current: 5.11 A | Power: 75.66 W
Time: 2.02 s | Current: 5.16 A | Power: 76.44 W
Time: 2.22 s | Current: 4.93 A | Power: 72.92 W
Time: 2.42 s | Current: 5.14 A | Power: 76.05 W
Time: 2.62 s | Current: 5.24 A | Power: 77.61 W
Time: 2.82 s | Current: 5.09 A | Power: 75.27 W
Time: 3.02 s | Current: 4.85 A | Power: 71.75 W
Time: 3.22 s | Current: 5.09 A | Power: 75.27 W
Time: 3.43 s | Current: 4.95 A | Power: 73.31 W
Time: 3.63 s | Current: 5.01 A | Power: 74.10 W
Time: 3.83 s | Current: 4.95 A | Power: 73.31 W
Time: 4.03 s | Current: 4.85 A | Power: 71.75 W
Time: 4.23 s | Current: 4.82 A | Power: 71.36 W
Time: 4.43 s | Current: 4.87 A | Power: 72.14 W
Time: 4.64 s | Current: 5.03 A | Power: 74.49 W
Time: 4.84 s | Current: 4.95 A | Power: 73.31 W
Time: 5.04 s | Current: 2.73 A | Power: 40.47 W
Time: 5.24 s | Current: -0.38 A | Power: -5.67 W
Time: 5.44 s | Current: -0.59 A | Power: -8.80 W
Time: 5.64 s | Current: -0.57 A | Power: -8.41 W
Time: 5.84 s | Current: -0.30 A | Power: -4.50 W
Time: 6.05 s | Current: -0.44 A | Power: -6.45 W
Time: 6.25 s | Current: -0.30 A | Power: -4.50 W
Time: 6.45 s | Current: -0.22 A | Power: -3.32 W
Time: 6.65 s | Current: -0.49 A | Power: -7.23 W
Time: 6.85 s | Current: -0.49 A | Power: -7.23 W
Time: 7.05 s | Current: -0.44 A | Power: -6.45 W
Time: 7.26 s | Current: -0.52 A | Power: -7.62 W
Time: 7.46 s | Current: -0.70 A | Power: -10.36 W
Time: 7.66 s | Current: -0.67 A | Power: -9.97 W
Time: 7.86 s | Current: -0.41 A | Power: -6.06 W
Time: 8.06 s | Current: -0.44 A | Power: -6.45 W
Time: 8.26 s | Current: -0.57 A | Power: -8.41 W
Time: 8.47 s | Current: -0.49 A | Power: -7.23 W
Time: 8.67 s | Current: -0.49 A | Power: -7.23 W
Time: 8.87 s | Current: -0.57 A | Power: -8.41 W
Time: 9.07 s | Current: -0.36 A | Power: -5.28 W
Time: 9.27 s | Current: -0.33 A | Power: -4.89 W
Time: 9.47 s | Current: -0.36 A | Power: -5.28 W
Time: 9.67 s | Current: -0.57 A | Power: -8.41 W
Time: 9.88 s | Current: -0.49 A | Power: -7.23 W

=== Energy Summary ===
Energy Used (Wh): 0.105
Energy Recovered (Wh): 0.009
Recovery Efficiency: 8.76 %
```

Figure 22: Prototype test (With RBS)

The next test scenario, the system was operated without any braking strategy following the motoring phase, allowing the motor to enter a coasting state. The test ran for 10 seconds, during which the motor was powered for approximately the first five seconds. After this period, the motor control inputs were disabled, and the motor was allowed to spin freely without any mechanical or electrical resistance applied via the controller. The purpose of this experiment was to measure the total energy consumed in an unassisted deceleration case and to confirm that no energy recovery occurs when braking is not implemented.

During the active motoring phase (0 to 5 seconds), the motor drew a steady current ranging between 6.20 A and 6.86 A, with power consumption ranging from 91 W to over 101 W. This reflects continuous battery discharge and significant energy use for acceleration or maintaining load. Following the transition to coasting at 5.0 seconds, the current dropped significantly to the range of 0.22 A to 0.59 A, and the power decreased to between 3.32 W and 8.80 W, likely reflecting idle system consumption and minor residual load from the motor's internal losses. However, most importantly, throughout the entire simulation duration, the current remained strictly positive, indicating that there was no reversal of current direction — a critical requirement for regenerative braking.

The energy summary confirms this observation: the total energy consumed during the simulation was 0.132 watt-hours, while the energy recovered was zero, resulting in a regeneration efficiency of 0.00%. Since the motor was allowed to coast freely rather than being subjected to active braking (such as dynamic or regenerative braking), no electromagnetic resistance was generated, and the motor’s kinetic energy dissipated entirely through mechanical losses. This outcome demonstrates that coasting alone does not contribute to energy recovery, even though it reduces energy usage compared to continuous motoring. Therefore, for systems aiming to improve efficiency via energy recapture, coasting must be replaced or supplemented by regenerative braking mechanisms that actively decelerate the motor and redirect current back into the energy storage system. (Shown in the figures below)

```
Time: 0.00 s | Current: 6.25 A | Power: 92.47 W
Time: 0.20 s | Current: 6.86 A | Power: 101.47 W
Time: 0.40 s | Current: 6.62 A | Power: 97.95 W
Time: 0.60 s | Current: 6.57 A | Power: 97.17 W
Time: 0.81 s | Current: 6.64 A | Power: 98.34 W
Time: 1.01 s | Current: 6.64 A | Power: 98.34 W
Time: 1.21 s | Current: 6.49 A | Power: 95.99 W
Time: 1.41 s | Current: 6.72 A | Power: 99.51 W
Time: 1.61 s | Current: 6.27 A | Power: 92.86 W
Time: 1.81 s | Current: 6.30 A | Power: 93.26 W
Time: 2.02 s | Current: 6.41 A | Power: 94.82 W
Time: 2.22 s | Current: 6.41 A | Power: 94.82 W
Time: 2.42 s | Current: 6.38 A | Power: 94.43 W
Time: 2.62 s | Current: 6.33 A | Power: 93.65 W
Time: 2.82 s | Current: 6.33 A | Power: 93.65 W
Time: 3.02 s | Current: 6.41 A | Power: 94.82 W
Time: 3.22 s | Current: 6.41 A | Power: 94.82 W
Time: 3.43 s | Current: 6.27 A | Power: 92.86 W
Time: 3.63 s | Current: 6.33 A | Power: 93.65 W
Time: 3.83 s | Current: 6.33 A | Power: 93.65 W
Time: 4.03 s | Current: 6.20 A | Power: 91.69 W
Time: 4.23 s | Current: 6.20 A | Power: 91.69 W
Time: 4.43 s | Current: 6.27 A | Power: 92.86 W
Time: 4.64 s | Current: 6.22 A | Power: 92.08 W
Time: 4.84 s | Current: 6.25 A | Power: 92.47 W
Time: 5.04 s | Current: 3.26 A | Power: 48.29 W
Time: 5.24 s | Current: 0.36 A | Power: 5.28 W
Time: 5.44 s | Current: 0.25 A | Power: 3.71 W
Time: 5.64 s | Current: 0.38 A | Power: 5.67 W
Time: 5.84 s | Current: 0.38 A | Power: 5.67 W
Time: 6.05 s | Current: 0.33 A | Power: 4.89 W
Time: 6.25 s | Current: 0.41 A | Power: 6.06 W
Time: 6.45 s | Current: 0.38 A | Power: 5.67 W
Time: 6.65 s | Current: 0.33 A | Power: 4.89 W
Time: 6.85 s | Current: 0.54 A | Power: 8.02 W
Time: 7.05 s | Current: 0.28 A | Power: 4.11 W
Time: 7.26 s | Current: 0.49 A | Power: 7.23 W
Time: 7.46 s | Current: 0.41 A | Power: 6.06 W
Time: 7.66 s | Current: 0.44 A | Power: 6.45 W
Time: 7.86 s | Current: 0.28 A | Power: 4.11 W
Time: 8.06 s | Current: 0.44 A | Power: 6.45 W
Time: 8.26 s | Current: 0.36 A | Power: 5.28 W
Time: 8.47 s | Current: 0.22 A | Power: 3.32 W
Time: 8.67 s | Current: 0.59 A | Power: 8.80 W
Time: 8.87 s | Current: 0.41 A | Power: 6.06 W
Time: 9.07 s | Current: 0.36 A | Power: 5.28 W
Time: 9.27 s | Current: 0.44 A | Power: 6.45 W
Time: 9.47 s | Current: 0.22 A | Power: 3.32 W
Time: 9.67 s | Current: 0.49 A | Power: 7.23 W
Time: 9.88 s | Current: 0.33 A | Power: 4.89 W

=== Energy Summary ===
Energy Used (Wh): 0.132
Energy Recovered (Wh): 0.000
Recovery Efficiency: 0.00 %
```

Figure 23: Prototype Test (No RBS)

3.3.1 Arduino code

The Arduino (15) Uno microcontroller was programmed to control the DC motor, simulate regenerative braking through directional reversal, and measure current to estimate both energy consumed and energy recovered. The source code is structured in a clear sequence: hardware setup, motor control by time intervals, current sensing, power calculation, and energy integration. Below is a detailed explanation of each section of the code.

```
// === Pin Definitions ===
const int IN1 = 8;
const int IN2 = 9;
const int CURRENT_SENSOR = A0;

// === Constants ===
const float Vref = 5.0;          // ADC reference
const float sensorOffset = 2.5; // ACS712 zero current voltage
const float sensitivity = 0.185; // V/A for ACS712 5A module
const float batteryVoltage = 14.8; // 4S Li-ion pack
const float batteryCapacityAh = 11.2;
```

Figure 24: Arduino code snippet

Figure 24 defines the hardware connections and essential constants. IN1 and IN2 are connected to the L298N motor driver's direction pins, while CURRENT_SENSOR is connected to the output of the ACS712 (3) current sensor. The constants define sensor calibration parameters (reference voltage, offset, and sensitivity) as well as battery characteristics for energy calculation. The offset of 2.5 V represents the sensor's no-current voltage output, and 0.185 V/A is the sensitivity for the 5A ACS712 variant.

```
unsigned long startTime;
unsigned long elapsedTime;

float totalUsedEnergy = 0.0;     // in Wh
float totalRecoveredEnergy = 0.0; // in Wh
```

Figure 25: Arduino code snippet

Figure 25, startTime stores the initial timestamp at the beginning of the simulation, while elapsedTime is continuously updated to track how many milliseconds have passed. Two float variables are initialized to accumulate the total energy used during motoring and the energy recovered during braking, both expressed in watt-hours (Wh)

```
void setup() {
  pinMode(IN1, OUTPUT);
  pinMode(IN2, OUTPUT);
  pinMode(ENA, OUTPUT);
  Serial.begin(9600);
  startTime = millis();
}
```

Figure 26: Arduino code snippet

In Figure 26, the setup() function runs once. It sets up the motor control pins (IN1, IN2, and ENA) as outputs, starts serial communication at 9600 baud for monitoring data, and records the starting time using millis().

```
void loop() {
  elapsedTime = millis() - startTime;

  // === 0–5 sec: Motoring ===
  if (elapsedTime < 5000) {
    digitalWrite(IN1, HIGH);
    digitalWrite(IN2, LOW);
    analogWrite(ENA, 200);
  }

  // === 5–10 sec: Braking ===
  else if (elapsedTime < 10000) {
    digitalWrite(IN1, LOW);
    digitalWrite(IN2, HIGH); // Reverse current = simulate regen
    analogWrite(ENA, 200);
  }

  // === Stop Motor ===
  else {
    digitalWrite(IN1, LOW);
    digitalWrite(IN2, LOW);
    analogWrite(ENA, 0);
    printResultsAndHalt();
  }
```

Figure 27: Arduino code snippet motor control

In Figure 27, this loop continuously checks the elapsed time and controls the motor accordingly. From 0–5 seconds, the motor rotates in the forward direction (motoring mode). From 5–10 seconds, the motor direction is reversed to simulate regenerative braking, and if the motor has momentum, the current may flow backward through the ACS712 (1) sensor. After 10 seconds, the motor is turned off and the final energy values are calculated and displayed.

```
// === Read Current ===
float current = readCurrent();
float power = batteryVoltage * current; // W

// === Track Energy ===
float deltaTime = 0.2 / 3600.0; // 200 ms = 0.2s, in hours
if (elapsedTime < 5000) {
  totalUsedEnergy += power * deltaTime;
} else if (elapsedTime < 10000) {
  if (current < 0) { // negative current = regen
    totalRecoveredEnergy += abs(power * deltaTime);
  }
}
```

Figure 28: Arduino code snippet current sensor

In Figure 28, the motor current is read from the sensor and converted into electrical power by multiplying it with the battery voltage (assumed constant). The time interval of 0.2 seconds is used to convert this into energy in watt-hours. Energy is accumulated separately for motoring and regenerative braking. During the motoring phase, all current is positive and contributes to totalUsedEnergy. In the braking phase, only negative current (regeneration) is counted in totalRecoveredEnergy.

```
Serial.print("Time: "); Serial.print(elapsedTime / 1000.0, 2);
Serial.print("s | Current: "); Serial.print(current, 2);
Serial.print(" A | Power: "); Serial.print(power, 2);
Serial.println(" W");
delay(200);
```

Figure 29: Arduino code snippet data print section

In Figure 29, this section prints the elapsed time, current, and power values to the serial monitor for real-time observation. A delay of 200 milliseconds regulates the sampling rate and matches the energy integration window used in calculations.

```
// === Read ACS712 Current Sensor ===
float readCurrent() {
  int raw = analogRead(CURRENT_SENSOR);
  float voltage = (raw / 1023.0) * Vref;
  float current = (voltage - sensorOffset) / sensitivity;
  return current;
}
```

Figure 30: Arduino code snippet data from ACS712 sensor

In Figure 30, this function reads the analog voltage from the ACS712 (1) sensor, converts it to a current using the known sensor sensitivity, and returns the result in amperes. This is used to compute power and energy in the loop.

```
78  // === Final Energy Summary ===
79  void printResultsAndHalt() {
80    Serial.println("\n=== Energy Summary ===");
81    Serial.print("Energy Used (Wh): ");
82    Serial.println(totalUsedEnergy, 3);
83    Serial.print("Energy Recovered (Wh): ");
84    Serial.println(totalRecoveredEnergy, 3);
85    float recoveryEfficiency = (totalRecoveredEnergy / totalUsedEnergy) * 100.0;
86    Serial.print("Recovery Efficiency: ");
87    Serial.print(recoveryEfficiency, 2);
88    Serial.println(" %");
89    while (1); // Stop loop
90  }
```

Figure 31: Arduino code snippet Final Summary Print Function

In Figure 31, this function prints the final energy summary to the serial monitor. It includes:

- Energy used during the motoring phase (Wh)
- Energy recovered during the regenerative braking phase (Wh)
- Efficiency percentage, calculated as:

$$Efficiency = \frac{Recovered\ Energy}{Used\ Energy} \times 100$$

The function ends with an infinite loop to halt further execution and lock the results on screen.

4. Results and Analysis

The results obtained from both simulation and real-life testing of the regenerative braking system reveal several key insights and important differences. In the simulation environment using MATLAB/Simulink, regenerative braking was modeled with idealized components such as a permanent magnet DC motor, a bidirectional power flow inverter, and a responsive lithium-ion battery block. These ideal components allowed for smooth and measurable transitions between motoring and regenerative braking phases. Notably, during the braking interval, reverse current was clearly observed, and the simulated battery's state of charge (SOC) increased, indicating successful energy recovery. Quantitatively, the simulation produced consistent energy recovery efficiencies ranging from 8% to 12% depending on the applied torque and braking duration. These outcomes validated the theoretical feasibility of regenerative braking in small electric vehicle systems and provided a clear energy benefit under controlled assumptions.

In contrast to the idealized simulation, real-life testing revealed notable differences in regenerative performance due to hardware limitations, particularly those associated with the L298N motor driver. While the simulation employed a fully bidirectional energy flow that allowed reverse current to recharge the battery, the L298N lacks true regenerative capability and cannot route recovered energy directly back into the battery system. However, despite this constraint, the prototype was able to demonstrate partial energy recovery through the presence of measurable back EMF generated during braking. The ACS712 (3) current sensor detected negative current values, confirming that the motor transitioned into generator mode and produced reverse current when braking torque was applied. This reverse current resulted in a small but consistent increase in the state of charge (SOC), with total energy recovery reaching approximately 8.76% of the energy used during the motoring phase. These findings suggest that while the L298N does not support efficient energy redirection, regenerative behavior is still partially achievable due to the motor’s inherent back EMF characteristics. This validates the potential of implementing regeneration even in constrained systems, though for practical and scalable energy recovery, upgrading to regenerative-capable motor drivers such as the BTS7960 or VESC is recommended to fully harness the recovered energy and improve system efficiency.

Another critical difference lies in the environmental and electrical behavior of real components. Unlike simulation, where motor parameters are linear and ideal, the actual DC motor exhibited non-linear current spikes during startup and coast-down phases. The

battery voltage remained mostly constant in simulation, whereas in real life, voltage fluctuations and internal resistance impacted current readings. Additionally, sensor inaccuracies, timing jitter in the Arduino (15), and measurement resolution limitations introduced minor inconsistencies in recorded data. Despite these issues, the prototype did validate the software's predictions in terms of general trends: high energy consumption during motoring, low or no recovery during braking, and the importance of control strategies.

Ultimately, this comparative analysis emphasizes the value of simulation for exploring design concepts and efficiency potential, while also highlighting the challenges of translating regenerative systems into practical, low-cost hardware implementations. It underscores the importance of choosing appropriate components and accounting for real-world imperfections when moving from theoretical modeling to physical experimentation.

4.1 Hardware Results

- The hardware prototype testing revealed that the regenerative braking system could successfully recover a measurable amount of electrical energy during deceleration. During the motoring phase (0–5s), current draw from the battery averaged between 4.85 A and 5.43 A, with corresponding power consumption around 70–80 W. This demonstrated consistent energy use while the motor was driving the load.
- Once regenerative braking was activated at 5 seconds, the L298N motor driver was switched into braking mode. The Arduino triggered the direction reversal, causing the DC motor to act as a generator. The ACS712 (1) current sensor detected negative current flow, with values ranging from −0.22 A to −0.70 A. These negative values confirmed that energy was being pushed back into the battery pack. The estimated energy recovered during braking was approximately 0.009 Wh, resulting in an overall recovery efficiency of 8.76% (18). Although modest, these results validated the regenerative function and provided a baseline for improvement.

4.2 Simulation Results

Simulations conducted using MATLAB/Simulink (10) showed consistent and predictable behavior that aligned closely with the theoretical expectations for a regenerative braking system. (9) In the first simulation scenario, the motor was operated for five seconds in motoring mode followed by five seconds of regenerative braking. During the motoring phase, the system's state of charge (SOC) steadily decreased as energy was consumed to drive the motor. Once braking was initiated, the simulation correctly reflected a reversal in current direction, and the SOC began to increase gradually. This behavior confirmed that the simulated system was effectively capturing the motor's back-EMF during deceleration and feeding the recovered energy back into the simulated battery model. Quantitative energy analysis revealed that approximately 4.48 joules were recovered from an initial energy consumption of 38.87 joules, resulting in a regeneration efficiency of 11.52%. (19) This level of efficiency is consistent with known values for low-voltage regenerative systems and demonstrates the potential benefit of incorporating energy recovery mechanisms into small electric vehicle (SEV) drive systems.

In a second simulation scenario where no braking torque was applied—allowing the motor to coast freely—SOC consistently declined throughout the entire 10-second test. No reverse current was observed, and no energy was recovered, clearly highlighting the difference between coasting and active regenerative braking (2). This comparison reinforces the notion that coasting, while reducing energy usage by eliminating power input, does not contribute to overall system efficiency through energy reclamation. Moreover, the simulation allowed for testing of different braking profiles. Gradual braking scenarios yielded more stable current and higher recovery efficiency compared to sudden, aggressive braking profiles, which caused current spikes and less efficient energy transfer due to abrupt system dynamics and losses. These variations demonstrate how braking strategy directly affects energy recovery performance.

Overall, the simulation results provided strong theoretical validation for regenerative braking under ideal conditions, and allowed for precise, measurable exploration of how torque, current, and SOC interact across different phases of operation. These findings serve as a benchmark for evaluating the limitations observed in the physical prototype

and emphasize the importance of optimized control logic and hardware selection when implementing regenerative braking in real-world systems.

5. Discussion

The successful demonstration of regenerative braking in both simulation and hardware highlights the practicality of implementing such systems in SEVs. The Arduino-based control logic and L298N (3) motor driver provided basic but functional control over braking behavior. Despite the L298N's limitations, such as thermal constraints and lack of direct energy routing capability, the system proved capable of initiating regeneration (20).

Key observations included the importance of braking profile on energy recovery, and the necessity of bypassing step-down converters (e.g., LM2596S) in the power path to preserve reverse current flow. Furthermore, using a current sensor like the ACS712 (1) allowed for real-time measurement of regenerative activity.

Areas for future enhancement include using a MOSFET-based H-bridge capable of higher efficiency and power handling, as well as integrating energy storage alternatives such as supercapacitors for improved performance during rapid braking. Incorporating smart battery management would further enhance safety and energy handling.

6. Conclusion and Recommendations

6.1 Conclusion

This study investigated the feasibility and performance of regenerative braking in small electric vehicles (SEVs) using both simulation and physical prototyping approaches. The simulation results demonstrated that regenerative braking can effectively recover a portion of the kinetic energy during deceleration, with energy recovery efficiencies ranging between 8% and 12% under ideal conditions. These results confirmed the theoretical benefit of incorporating regenerative braking into lightweight, low-voltage systems such as e-scooters or e-bikes. However, real-world testing highlighted significant practical limitations, particularly due to hardware constraints. The use of the L298N (3) motor driver, which lacks true bidirectional energy flow capability, restricted the system to dynamic braking only. As a result, no actual energy recovery was recorded during braking, and the battery's state of charge continued to decrease, revealing a gap between simulation potential and physical realization.

Despite these limitations, the prototype successfully demonstrated current monitoring, energy tracking, and the basic control logic needed for regenerative operation. It also emphasized the importance of component selection in achieving functional regenerative systems. Based on these findings, several recommendations can be made for future improvements. First, replacing the L298N (3) with a regenerative-capable driver such as the BTS7960, VNH2SP30, or a VESC would enable true energy feedback into the battery. Second, integrating a more advanced battery management system (BMS) with current-limiting and charge acceptance control would allow for safe and efficient energy recovery. Additionally, refining the control algorithm to dynamically adjust braking torque based on speed and battery SOC could improve performance and prevent overcharging. Finally, future studies should explore extended testing under varied load conditions and implement energy storage alternatives such as supercapacitors to evaluate hybrid recovery strategies. Overall, this project establishes a strong foundation for further development of low-cost, energy-efficient regenerative braking solutions in light electric mobility systems.

6.2 Recommendations

- Replace the L298N (3) with a high-efficiency MOSFET-based motor driver for better current handling and thermal management.
- Integrate smart battery management to monitor state-of-charge and temperature, improving energy absorption and safety.
- Use supercapacitors in conjunction with the battery to absorb sharp regenerative spikes.
- Extend prototype testing to include different braking profiles and motor speeds for broader performance validation.
- Explore wireless data logging from the Arduino (15) for long-term energy tracking and diagnostics.

To improve the performance and efficiency of regenerative braking systems in small electric vehicles (SEVs), several technical enhancements are recommended based on the limitations identified during prototype testing. First, the L298N (3) motor driver should be replaced with a high-efficiency MOSFET-based motor driver, such as the BTS7960 or VESC, which are designed for higher current handling and improved thermal management. Unlike the L298N, which suffers from significant voltage drops and lacks regenerative capabilities, MOSFET-based drivers offer lower resistance, higher switching efficiency, and support for bidirectional current flow—enabling actual energy recovery into the battery. Second, the system should be paired with a smart battery management system (BMS) that can monitor parameters such as state of charge (SOC), temperature, and charging current limits in real time. This not only ensures optimal energy absorption during regeneration but also prevents battery damage and thermal runaway during rapid braking cycles. Third, to address the challenge of handling sharp regenerative current spikes, it is recommended to integrate supercapacitors in parallel with the battery. Supercapacitors can absorb and release energy quickly, reducing stress on the battery during short, high-intensity regenerative events, and improving the overall efficiency and durability of the energy storage system.

In addition to hardware upgrades, further experimental testing should be expanded to include a variety of braking profiles—including sudden, gradual, and pulsed deceleration—as well as tests at different motor speeds and loads. This would allow for a more comprehensive evaluation of the system's regenerative performance across real-world operating conditions and contribute to optimizing the braking control logic. Lastly, implementing wireless data logging capabilities, such as Bluetooth or Wi-Fi modules connected to the Arduino (15), would enable long-term monitoring of current, voltage, and energy data without physical tethers. This feature would be especially useful for tracking performance trends over multiple charge cycles, identifying inefficiencies, and diagnosing hardware issues in live environments. Together, these recommendations aim to enhance the functionality, safety, and energy efficiency of SEV regenerative braking systems and move them closer to practical deployment in urban mobility applications.

References

1. Microsystems A. ACS712 Hall-Effect Current Sensor Datasheet. Worcester, MA: Allegro Microsystems; 2017.
2. A K, MS F, A G. Electric and Hybrid Vehicles: Technologies, Modeling and Control – A Mechatronic Approach. Hoboken: Wiley; 2014.
3. STMicroelectronics.. L298N Dual Full-Bridge Driver Datasheet Geneva: STMicroelectronics; 2020.
4. CJ VD. Regenerative Electric Railway System. Massachusetts: U.S. Patent No. 889,938; 1908.
5. KT C. Electric Vehicle Machines and Drives: Design, Analysis and Application Hoboken: Wiley; 2015.
6. Larminie J LJ. Electric Vehicle Technology Explained. 2nd ed. Hoboken: Wiley; 2012.
7. TD G. Fundamentals of Vehicle Dynamics Warrendale: Society of Automotive Engineers; 1992.
8. N L. System Dynamics for Engineering Students: Concepts and Applications. 2nd ed. San Diego: Academic Press; 2017.
9. III PW. MATLAB/Simulink for Engineering Applications. 4th ed. New York: McGraw Hill Education; 2020.
10. MathWorks. Simscape Electrical Specialized Power Systems documentation Natick (MA): MathWorks; 2023.
11. I D, HS H. Energy Efficiency and Management in Electric Vehicles. Cham: Springer; 2017.
12. Dincer I HH. Energy Storage Systems for Renewable Energy Applications London: Academic Press; 2017.
13. D O. Urban Mobility Trends in Ulaanbaatar: Case Study on E-Scooters Ulaanbaatar: Ulaanbaatar Daily; 2022.
14. Mongolia NSOo. Transport Sector Statistical Report Ulaanbaatar: NSO; 2023.

15. Banzi M SM. Getting started with Arduino: The open source electronics prototyping platform. 3rd ed. Sebastopool: Maker Media; 2014.

16. Mabuchi Motor Co. L. 550VC-8021F DC Motor Datasheet Tokyo: Mabuchi Motor; 2023.

17. SJ C. Electric machinery fundamentals. 5th ed. New York: McGraw-Hill; 2011.

18. Mohan S KRSA. Implementation and Analysis of Regenerative Braking System in Electric Bicycle: Int J Eng Res Technol (IJERT); 2020.

19. Kumar V KR. Estimation of energy recuperation in electric two-wheelers through regenerative braking: J Energy Storage; 2021.

20. Arshad R MS. Comparative analysis of H-bridge driver ICs for regenerative braking in small EVs: Electron Rev; 2019.

21. I H. Electric and Hybrid Vehicles: Design Fundamentals. 2nd ed. Boca Raton: CRC Press; 2011.

22. Ehsani M GYEA. Modern Electric, Hybrid Electric, and Fuel Cell Vehicles. 3rd ed. Boca Raton: CRC Press; 2018.

23. Mi C MMGD. Hybrid Electric Vehicles: Principles and Applications with Practical Perspectives Hoboken: Wiley; 2011.

24. Chen Z MCZJ. Comparison of electric vehicle regenerative braking strategies on battery life and energy efficiency: IEEE Trans Veh Technol; 2015.

25. Piller S PMJA. Methods for state-of-charge determination and their applications: J Power Sources; 2001.

26. Gammack J HM. Internet of things and data analytics handbook Amsterdam: Elsevier; 2021.